Can VIP be an Alternative Solution for Energy Retrofit for Enhancing the Thermal Performance of Wood-Frame Walls?

Hamed H. Saber, PhD **Wahid Maref, PhD** *Member ASHRAE* **Ganapathy Gnanamurugan** **Mike Nicholls**

ABSTRACT

Field monitoring of the dynamic heat transmission characteristics of residential 2 × 6 wood-frame wall systems that had been retrofitted using vacuum insulation panels (VIPs) with glass fiber cores and extruded polystyrene foam (XPS) panels were undertaken in 2011–2012 at the Field Exposure of Walls Facility (FEWF) of the NRC Construction. The main objective of this research was to evaluate the steady-state and transient thermal performance of three wall assemblies (4 ft × 6 ft), two of which incorporated VIPs within an XPS tongue and groove (T&G) configuration and VIPs within an XPS clip-on (C-O) configuration, and a third assembly incorporating only XPS. The three wall assemblies were installed in the FEWF for one year cycle of exposure to outdoor natural weather conditions. The NRC's hygrothermal model, hygIRC-C, was validated against the measured data. Results showed that the model predictions were in good agreement with the experimental data. Given that the VIP could be punctured during the installation process (e.g., inadvertent use of fasteners in wall assembly) or may fail during normal operating conditions or due to imperfection during the manufacturing process, the numerical model was used to conduct parametric analyses in order to predict the thermal resistance (R-value) in cases where one or more VIPs failed.

In the final phase of this study, the model was used to predict the yearly cumulative heat losses from the respective wall systems. It is important to point out that the aging effect and the effect of the thermal bridging due to the envelope (i.e., skin) of the VIPs are not accounted for in this study. However, sensitivity analysis of the thickness and thermal conductivity of the VIP envelope was conducted in this paper to investigate the effect of these parameters on the effective R-values of VIP. Results showed that the yearly cumulative heating loads for the XPS retrofit wall specimen was 69.9% and 78.8%, respectively, greater than that obtained for the T&G VIP retrofit wall specimen and the C-O VIP retrofit wall specimen. Furthermore, the results showed that the effect of the furred-airspace assembly in the C-O VIP retrofit wall specimen when the emissivity of all surfaces that bounded the airspace was assumed to be 0.9 resulted in a reduction in the yearly heating load by 5% compared to the T&G VIP retrofit wall specimen without furred-airspace.

INTRODUCTION

Increasingly, home builders are turning towards a variety of construction and retrofit methods to improve thermal performance whilst reducing the operating cost of buildings. The energy crisis in the 1970s had a major effect on building technology related to energy performance. Thermal insulation of buildings became the key element to minimize heat losses, hence improving the energy performance. Adding more thermal insulation on the exterior wall and increasing the airtightness of the assembly was an evident solution adopted by many practitioners to achieve reduced energy usage in homes. In order to achieve better airtightness, high levels of envelope insulation will certainly be required with wall thermal resistances (R-values) of more than 3.33 $m^2 \cdot K/W$ (18.9 $ft^2 \cdot h \cdot °F/Btu$) and roof R-values of more than 5.0 $m^2 \cdot K/W$ (28.4 $ft^2 \cdot h \cdot °F/Btu$)

Hamed H. Saber *is a research officer,* ***Wahid Maref*** *is a senior research officer, and* ***Ganapathy Gnanamurugan*** *and* ***Mike Nicholls*** *are technical officers at NRC Construction, National Research Council Canada. Ottawa, Ontario.*

(Maref et al. 2011, 2012a). Normally, the air leakage and airtightness across the wall systems depends on the type of insulation materials, air-barrier systems, and the pressure differential across the wall systems (Maref et al. 2011, 2012a; Elmahdy et al. 2009, 2010; Saber et al. 2010a, 2012a).

To achieve high levels of energy performance with existing wall systems and materials, the wall systems would need to be considerably thicker and this may be less acceptable to consumers because of the loss of usable floor area, greater weight, increase in costs due to transportation, and time of construction, as well as new challenges for the structure associated with greatly increased wall thickness. To maintain reasonable envelope thickness while having high thermal performance, a promising recent innovation in building technology was investigated within the context of its application using Vacuum Insulation Panel (VIP) systems. Due to high R-values per unit thickness of VIPs, their potential is considered to be a promising means of insulating the building envelope to high levels of thermal resistance. By considering the center of the panel, VIPs are of interest owing to their exceptional insulating R-value, up to 10.6 $m^2 \cdot K/W$ (60 $ft^2 \cdot h \cdot °F/Btu$) per inch or even higher (Ogden and Kendrick 2005; Maref et al. 2011, 2012a). This concept is gaining interest and is being considered by architects and building practitioners for new and retrofit construction (Mukhopadhyaya 2010). In the case of accounting for the thermal bridging due the envelope (i.e., skin) of the VIP, the effective R-value might be lower than that at the center of the panel.

Despite their high R-values at the center of the panels, VIPs have been slow to make inroads into construction because of three drawbacks: cost, the need to protect them against puncturing, and the absence of long-term performance data or procedures to predict their long-term performance. Recently, Canadian, European, and Chinese research efforts have mainly focused on the core materials and the envelopes of the VIPs themselves (Cremers 2005; Mukhopadhyaya 2006; Mukhopadhyaya et al. 2008, 2009; Simmler and Brunner 2005a, 2005b; Brunner and Simmler 2008; Stahl et al. 2012; Schwab et al. 2005; Ghazi Wakili et al. 2004; Xiaobo et al. 2013). Also, research has now started to investigate how to integrate VIP insulation in building construction in such a way that the thermal advantages are fully used. Preliminary efforts have been published in IEA Annex 39 on High Performance Thermal Insulation (IEA Annex 39 2005).

The VIP technology can be used in retrofitting the existing homes, for example, either at the interior or at the exterior of the wall assemblies (Binz and Steinke 2005; Rogatzki 2009). It can also be used in new construction such as wood-frame construction in double stud walls (Maref 2011; Haavi et al. 2012). Most of the VIP activities in Canada are still in the research and development phase with some demonstration projects that have been recently completed (Maref et al. 2011, 2012a). Germany and Switzerland are the first two countries where VIP technology has been introduced to the building construction sector, through research efforts such as those of the IEA Annex 39 (2005).

Cremers (2005) pointed out that since VIP technology is considerably more costly than established insulating technologies, in the future measures such as improved production capacity, efficient manufacturing techniques, and alternative and less expensive core material of the VIP will likely contribute in making VIP insulation more cost-effective for building envelopes. Several prototype projects have been completed or are being carried out in Europe using VIP technology (IEA Annex 39 2005). Further technology developments in the area of insulation technology and recent global concerns about climate change phenomena showed that there is room and need for improvement in the insulation technology for building envelopes. Hence, the National Research Council (NRC) of Canada and other organizations and laboratories around the world have established research programs and studies that focused on the applicability of high performance VIPs in building envelope construction.

OBJECTIVE

Based on PERD (Program on Energy Research and Development) research efforts on "Next Generation Building Envelope Building Systems" by NRC, Natural Resources Canada (NRCan), and Canada Mortgage and Housing Corporation (CMHC), it appears that VIP-based insulation systems are capable of reducing building energy consumption in Canada (Maref et al. 2011, 2012a). The main objective of this paper is to use a numerical model in order to evaluate the dynamic heat transmission characteristics of three mid-scale 2×6 wood-frame wall assemblies, two of which incorporated VIPs within an XPS tongue and groove (T&G) configuration and VIPs within an XPS clip-on (C-O) configuration, and a third assembly incorporating only XPS, in the Field Exposure of Walls Facility (FEWF) of NRC Construction, located in Ottawa for one year cycle of exposure to outdoor natural weather conditions. The numerical model was validated against the measured data. The measured data was obtained from field monitoring of the dynamic heat transmission characteristics of these wall systems that were tested in period between May 2011 and May 2012 in the FEWF. Given the fragile nature of VIPs (they could be punctured during the installation process or may fail during normal operating conditions), the numerical model was used to conduct parametric analyses to predict the R-value in cases where one or more VIPs failed. Also, the model was used to investigate the reduction in R-value of walls incorporating VIPs when one or more VIPs were replaced by XPS layer of the same thickness as the VIP. Finally, the model was used to predict the yearly cumulative heat losses from the respective wall systems.

DESCRIPTION OF RETROFITTED WALL SPECIMENS

Three wall specimens (4 ft × 6 ft) conforming to typical residential wood-frame construction were installed side-by-side in the FEWF. The different material layers and the dimensions of the wall specimens are shown in Figures 1 and 2. The backup wall for all three retrofit strategies consists of interior drywall (1/2 in. thick), polyethylene air barrier (6 mil), 2 × 6 wood-frame with friction-fit glass fibre batt insulations, OSB (7/16 in. thick), and Tyvek sheathing membrane. The backup wall was retrofitted by adding different types of external insulations. The first wall (W1) was retrofitted by adding an XPS layer (2 in. thick) between the sheathing membrane and vinyl siding. The other two walls were retrofitted with vacuum insulation panels (VIPs) using two concepts as described below. No information is available about the type of the material of the VIP envelope (i.e., skin) and the degree of vacuum inside the VIP.

In the second retrofit concept, each VIP having nominal thickness of 15 mm (5 panels in total) was sandwiched between an exterior XPS board (1 in. thick) and an interior XPS board (5/8 in. thick). Note that VIPs of thickness of 20 mm and thicker up to 40 mm are common in Germany and Switzerland. To protect the VIP, a hollow piece of XPS of the same thickness as the VIP was cut and the VIP panel was placed inside the opening such that the VIP would be protected by the XPS surround. The effect of thermal bridging of the XPS surround on the effective R-value of the wall assembly was accounted for by the numerical model. The assembly consisting of the VIP and XPS surround was placed between the exterior and interior XPS layers to form a tongue and groove (T&G) VIP "sandwich," as shown in Figure 3. A thin glue layer was applied on the surfaces of the VIP to ensure good contact between the VIP and the XPS layers. Five T&G VIP sandwiches were assembled (friction-fit at the tongue and groove interfaces, see Figure 3c). Then the entire assembly of T&G VIPs was placed vertically between the sheathing and smart board for the retrofitted wall specimen. The smart board used in study, called *waferboard*, is a class of mat-formed structural panels made predominantly of wood wafers.

In the third retrofit concept (see Figure 4), the VIP sandwich was similar to the VIP sandwich described in the second concept but without the tongue and groove assembly. In this concept, five VIP sandwiches were assembled using clips. Hence, the retrofitted wall specimen was called clip-on (C-O) VIP. To ensure good contact, a foamed polychloroprene (neoprene) gasket was inserted between the VIP sandwiches as shown in Figure 4. The C-O VIP assembly was stacked vertically against the surface of the sheathing membrane. Vertical furring strips (16 inch o.c. and 5/8 inch thick) were attached to metal clips, which supported the C-O VIP assembly and provided the nailing surface to which the smart board (waferboard) was attached. Detailed descriptions for the instrumentation (i.e., thermocouples, heat flux transducers, pressure sensors, and RH sensors) of the reference wall (W1), the C-O VIP (W2), and the T&G VIP (W3) are available in Maref et al. (2012b). As a part of the test protocol, all thermocouples used in the three test specimens were calibrated. Also, all heat flux transducers were calibrated according to the ASTM C-1130 *Standard Practice for Calibrating Thin Heat Flux Transducers* (ASTM 2009). The uncertainties of temperature and heat flux measurements were ± 0.1°C and ±5%, respectively.

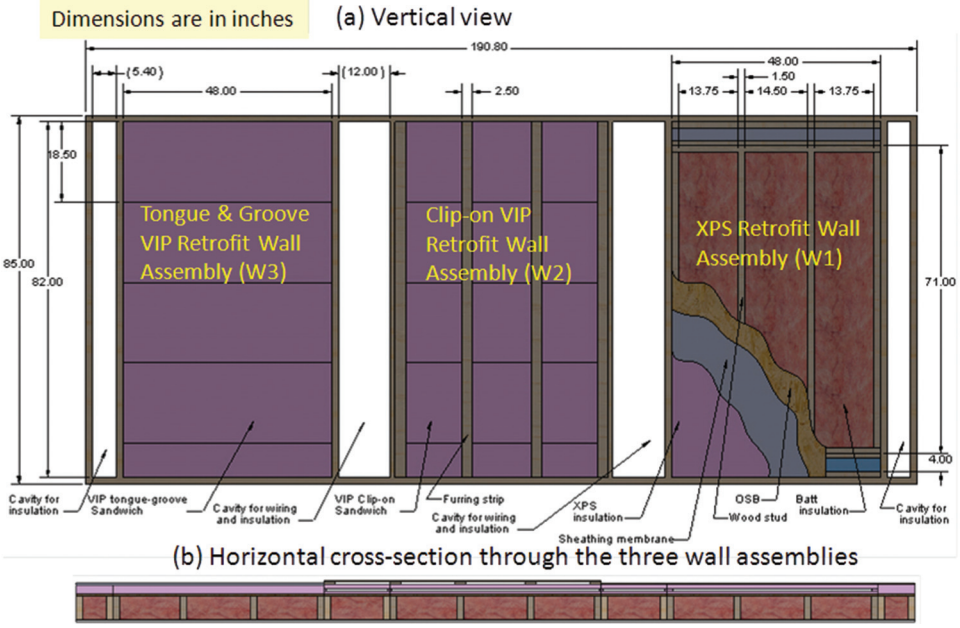

Figure 1 *Schematic of three residential 2 in. × 6 in. wood-frame wall test specimens installed side by side in the Field Exposure of Walls Facility (FEWF) of NRC Construction.*

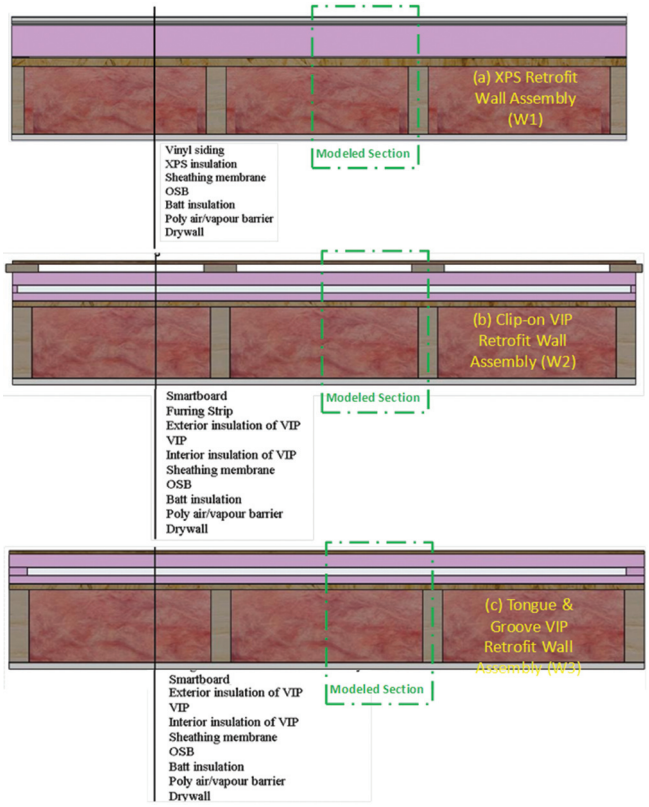

Figure 2 *Horizontal cross-section through different wall systems.*

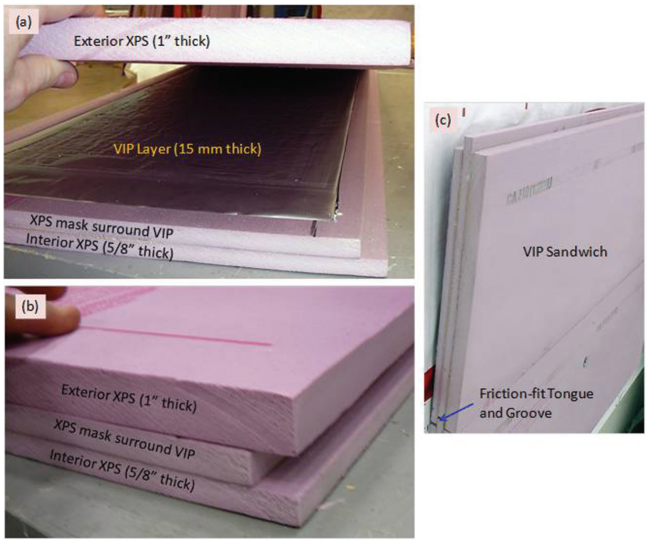

Figure 3 *Tongue and groove (T&G) VIP assembly (W3).*

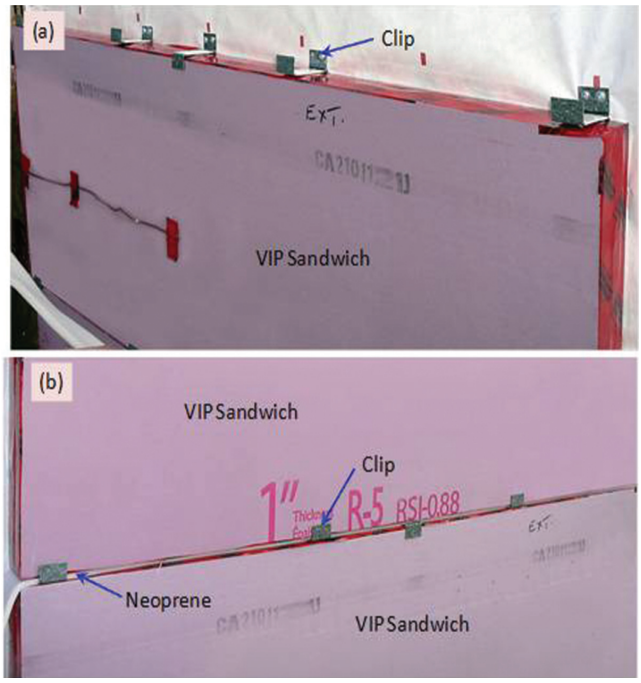

Figure 4 *Clip-on (C-O) VIP assembly (W2).*

MODEL DESCRIPTION AND VALIDATION

The numerical model that was used in this study simultaneously solves the highly nonlinear 2D and 3D heat, air, and moisture (HAM) equations. This model has been extensively validated in a number of other projects and has been used in several related studies to assess the thermal and hygrothermal performance of wall and roofing systems (Elmahdy et al. 2009, 2010; Saber and Swinton 2010; Saber and Laouadi 2011; Saber et al. 2010 a, 2010b, 2010c, 2011a, 2011b, 2011c, 2012 a, 2012b, 2012c, 2012d; Armstrong et al. 2011a, 2011b; Saber and Maref 2012; Saber 2012, 2013). The 3D version of this model was used to conduct numerical simulations for different full-scale wall assemblies incorporating, or not, penetrations representative of a window installation, such that the effective R-value of the assemblies could be predicted, taking into consideration air leakage across the assembly. The predicted R-values for these walls, which incorporated different types of spray polyurethane foams or glass fiber insulation, were in good agreement (within ±5%) with the measured R-values that were obtained from testing in a guarded hot box (GHB) (Elmahdy et al. 2009, 2010; Saber et al. 2010a, 2012a).

The present model was also validated against GHB test results (Saber et al. 2011a) and then used to conduct numerical simulations to investigate the effect of foil emissivity on the effective thermal resistance of different wall systems with foil bonded to different types of thermal insulations placed in furred assemblies, in which the foil was adjacent to the airspace (Saber and Swinton 2010; Saber and Maref 2012; Saber

et al. 2012b). Also, the present model was validated and used to assess the thermal performance of insulated concrete form (ICF) wall systems when placed in the FEWF and subjected to yearly periods of Canadian climate (Saber et al. 2010c, 2011c; Armstrong et al. 2011a, 2011b). In these studies (Elmahdy et al. 2009, 2010; Saber and Swinton 2010; Saber et al. 2010a, 2010c, 2011a, 2011c, 2012a, 2012b; Saber and Maref 2012; Armstrong et al. 2011a, 2011b), no moisture transport was accounted for in predicting the thermal performance of different types of walls.

In instances where the model was used to account for moisture transport across wall assemblies, this model predicted the drying rate of a number of wall assemblies subjected to different outdoor and indoor boundary conditions (Saber et al. 2010b) in which there was a significant vapour drive across the wall. The results showed that there was overall agreement between the results derived from the present model and the hygIRC-2D model, a model that had been previously developed and validated at the NRC (Maref et al. 2002). The present model predictions were in good agreement with the experimental measurements of the drying and drying rate of the assembly in respect to the shape of the curve and the length of time predicted for drying. As well, the predicted average moisture content of the different wall assemblies over the test periods were in good agreement, all being within ±5% of those measured (Saber et al. 2010b). Furthermore, in respect to the prediction of the hygrothermal performance of roofing systems, the present model was used to investigate the moisture accumulation and energy performance of reflective (white) and non-reflective (black) roofing systems that were subjected to different climatic conditions of North America (Saber et al. 2011b, 2012d).

Having previously validated the present model against experimental data of several tests undertaken in controlled laboratory conditions, a subsequent and important step in this study was to validate the present model against field measurements. Thereafter, the general parameters affecting the thermal response of wall specimens is discussed, information is provided regarding assumptions, and initial and boundary conditions that were used in conducting the numerical simulations. Finally, the estimated yearly cumulative heating and cooling loads by the model due to the respective wall specimens are discussed.

GENERAL PARAMETERS AFFECTING THE THERMAL RESPONSE OF WALL SPECIMENS

The thermal response of the wall specimens depends on both the thermal properties of all material layers of the wall specimens and the outdoor and indoor conditions. All thermal properties of the different layers of which the wall assemblies were composed, with the exception of the vacuum insulation panels (VIPs), were taken from *ASHRAE Handbook of Fundamentals* (ASHRAE 2009). However, the properties of the VIPs had been previously characterized in another project (see references Maref et al. [2011, 2012a] for more details). The thermal conductivity of the VIP layer was measured at different temperatures. Two specimens of VIP having a nominal thickness of 15 mm and length and width of 1200 mm and 455 mm, respectively, were used to measure the thermal conductivity at three mean temperatures. The measured density of the VIP samples was 261.2 kg/m^3. It is important to point out that the type of the VIP that was used in this project is proprietary product. The details about the composition of this type of VIP are not available (such as degree of vacuum inside the VIP, type of fiber core material inside the VIP, and type of material and its thickness of the VIP envelope).

The test method used to measure the thermal conductivity of the VIP was ASTM C-518 (ASTM 2007). The use of heat flowmeter apparatus according to the ASTM C-518 test method when there are thermal bridges present in the assembly may yield results that are unrepresentative of the assembly (see ASTM [2007] for more details). According to the ASTM C-518 test method (ASTM 2007), the thermocouples embedded in the surfaces of the upper and lower plates (12 × 12 in. ([305 × 305 mm]) of the heat flowmeter measure the temperature drop across the specimen and the heat flux transducer (HFT) embedded in each plate measures the heat flow through the specimen. The size of HFT in the NRC's heat flowmeter is 6 × 6 in. (152 × 152 mm). The uncertainty of the measurements in this test method is ±2%. As indicated earlier, the size of the VIP sample is 1200 × 455 mm, which is larger than the size of upper and bottom plates of the heat flowmeter (305 × 305 mm). As such, the measured R-value of the VIP using the heat flowmeter is not the effective R-value because the effect of thermal bridging due to the VIP edges is not accounted for. The limitations of using the test method of ASTM C-518 (ASTM 2007) for measuring the R-values of samples with thermal bridging are recently addressed by Saber (Saber 2012; Saber at al. 2012c). Alternatively, the ASTM C-1363 test method using the GHB can be used to determine the effective thermal resistance of samples with thermal bridges (ASTM 2006).

In this paper, the values of the thermal resistance and the corresponding thermal conductivity of the VIP are applicable to the center core of the VIP only. These values are applicable to whole VIP only in one case when the thermal conductivity of VIP envelope is the same as the thermal conductivity of the center core of the VIP. Figure 5 shows the dependence of the thermal conductivity of the center core of the VIP samples on the temperature. The measured thermal conductivity of VIP layer, λ in W/(m·K), as a function of temperature, T in °C, that was used in the numerical simulation is given as:

$$\lambda = a + b \times T,\ a = 0.002054,\ b = 7.03088 \times 10^{-6} \qquad (1)$$

The above correlation of λ is in good agreement with all measured values at different temperatures (within ±1.6%). The corresponding average R-value of the center core of the VIP sample (15 mm thick) is 7.03 m^2·K/W (39.9 ft^2·h·°F/Btu).

To quantify the effect of the thermal bridging due to the envelope of the VIP on its effective R-value, 2D numerical

simulations were conducted for VIPs of 15 mm thick, different heights (H) of 400 mm and 800 mm, and different envelope thicknesses (δ_{skin}) of 0.1 mm and 0.2 mm. The 2D numerical simulations represent the case of using VIP of a large width. In these simulations, the thermal conductivity of the VIP core was taken equal to the measured value using the ASTM C-518 test method (0.00214 W/[m·K]), whereas a wide range was considered for the thermal conductivity of the VIP envelope (ranging from 0.00214–10.0 W/[m·K]). Figure 6 shows the dependence of the effective R-values of the VIP (R_{VIP}) of different H and δ_{skin} on the thermal conductivity of its envelope (λ_{skin}). As shown in this figure, the parameters H, λ_{skin}, and δ_{skin} have a significant effect on the effective R-value of the VIP. For example, for VIP of δ_{skin} = 0.2 mm and H = 400 mm, the R_{VIP} decreases by 33% (from 39.9 ft^2·h·°F/Btu to 30.0 ft^2·h·°F/Btu) as λ_{skin} increases from 0.00214 W/(m·K) to 1.0 W/(m·K). At λ_{skin} = 1.0 W/(m·K) and H = 400 mm, increasing δ_{skin} from 0.1 mm to 0.2 mm resulted in a decrease in the R_{VIP} by 13% (from 33.8 ft^2·h·°F/Btu to 30 ft^2·h·°F/Btu). Furthermore, at λ_{skin} = 1.0 W/(m·K) and δ_{skin} = 0.1 mm, increasing H from 400 mm to 800 mm resulted in an increase of R_{VIP} by 7.4% (from 33.8 ft^2·h·°F/Btu to 36.3 ft^2·h·°F/Btu). In summary, the results shown in Figure 6 clearly indicated that the thermal bridging due the envelope of the VIP can have a significant effect on its effective R-value. This effect, however, was neglected in this study due to lack of information about the envelope of the VIP. Also, due to lack of information about the change of the degree of vacuum inside the VIP with time, the aging effect on the effective R-value was not accounted for in this study.

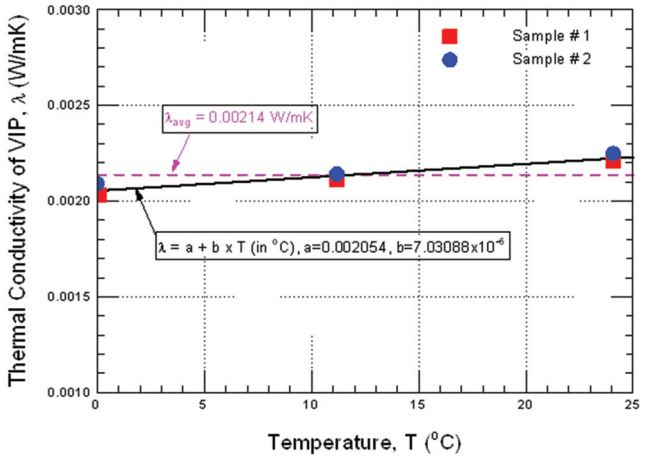

Figure 5 *Measured thermal conductivity at the center core of the VIP samples (15 mm thick).*

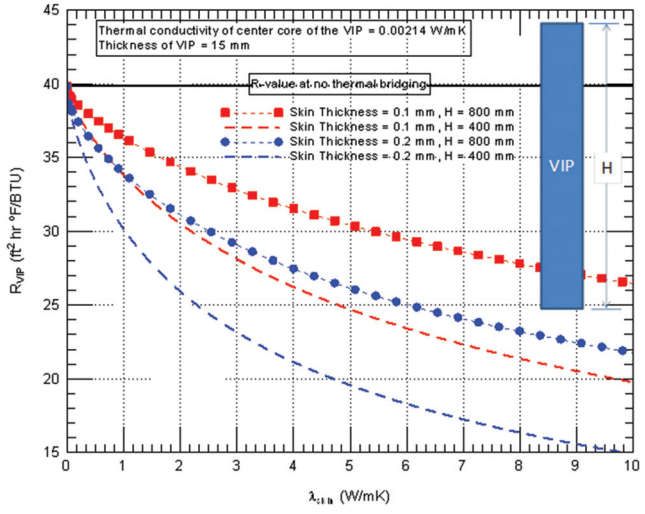

Figure 6 *Effect of thermal bridging due to VIP envelope on its effective R-value.*

The thermal conductivity and R-value of the VIP were also measured using the ASTM C-518 test method (ASTM 2007) when the VIP failed. These measurements were conducted in order to investigate the reduction in R-value of a retrofitted wall specimen incorporating VIPs for which one or more VIPs failed. The measured values of thermal conductivity and R-value when the VIP failed were 0.0257 W/(m·K) and 3.32 ft^2·h·°F/Btu, respectively. It is important to point out that the thermal conductivity of the VIP when it failed is approximately equal to the thermal conductivity of still air. Furthermore, when the VIP failed, its thermal conductivity is significantly increased by a factor of ~12 (increased from 0.00214 W/[m·K] to 0.0257 W/[m·K]); and this resulted in a significant reduction in its R-value (from 39.9 ft^2·h·°F/Btu to 3.32 ft^2·h·°F/Btu). Consequently, consideration and care should be given in handling and installing VIPs in the wall systems so as to minimize the risk of puncturing them. The present model was used to predict the steady-state and transient thermal performance of different wall systems (W1, W2, and W3).

ASSUMPTIONS

It was assumed that all material layers are in perfect contact (i.e., the interfacial thermal resistances between all material layers were neglected). Due to lack of information about the type of VIP that was used in this project, the effects of aging and thermal bridging due to the envelope of the VIP were neglected. Note that the constructive thermal bridges in the different wall systems (W1, W2, and W3) were obviously considered in this study. The emissivity of all surfaces that bounded the airspaces (i.e., airspaces between XPS layer and vinyl siding for W1 and airspaces between vertical furring, C-O VIP assembly, and waferboard for W2) was taken equal to 0.9 (ASHRAE 2009). The effect of heat transfer by conduction, convection, and radiation inside these airspaces on the thermal performance of W1 and W2 are accounted for.

INITIAL AND BOUNDARY CONDITIONS

The initial temperature in all material layers of specimens W1, W2, and W3 was assumed uniform and equal to 10.0°C. Since this initial temperature was not the same as in the test, it was anticipated that the predicted dynamic response of the different wall specimens in the first period of the test (say first 24–48 h) would be different from that obtained in the test itself. Due to symmetry, only one module of each wall system was modeled, which is formed from a vertical plane passing through the middle of the stud and a vertical plane passing through the middle of the stud cavity (see the green dashed boxes shown in Figure 2a, b, c). The boundary conditions on these vertical planes are adiabatic due to symmetry. The boundary conditions on the top and bottom surfaces of one module of the wall systems are adiabatic (i.e., no edge heat losses).

In this study, two types of numerical simulations were conducted:

- Steady-state numerical simulations to determine the R-values of different wall specimens. In this case, the outdoor surface of the vinyl siding for W1 and smart board (waferboard) for W2 and W3 were subjected to convective boundary conditions with an air temperature of –35°C and heat transfer coefficient of 34.0 W/(m^2·K) (ASTM 2006). Similarly, the indoor surface of the gypsum board for all wall systems was subjected to a convective boundary condition with constant air temperature and heat transfer coefficient of 21.0°C and 8.29 W/(m^2·K), respectively (ASTM 2006). The boundary conditions on the outdoor and indoor surfaces of the wall specimens are similar to the case of measuring the R-value using the guarded hot box (GHB) in accordance with ASTM C-1363 test method (ASTM 2006).
- Transient numerical simulations were conducted in order to validate the present model and then determine the yearly heating and cooling loads for different wall specimens. In this case, the outdoor surface of the vinyl siding for W1 and smart board (waferboard) for W2 and W3 were subjected to temperature boundary conditions. Similarly, the indoor surface of the gypsum board for all wall systems was subjected to a temperature boundary condition. The temperatures on the outdoor and indoor surfaces of different wall specimens (changed with time) were taken equal to that measured on these surfaces (see reference Maref et al. [2012b] and Saber et al. [2012e] for more details). As an example, these temperatures are shown in Figure 7 for wall W1.

THERMAL RESISTANCES OF DIFFERENT WALL SPECIMENS

As indicated earlier, the present model was extensively validated in previous studies (Elmahdy et al. 2009, 2010; Saber 2012a, 2010a; Saber 2012; Saber et al. 2012c) by comparing the predicted R-values against the measured R-values obtained using two standard test methods: (a) guarded hot box in accordance with ASTM C-1363 (ASTM 2006), and (b) heat flowmeter in accordance of ASTM C-518 (ASTM 2007). Results showed that the predictions of the present model were in good agreement with the experimental data (within the uncertainties of the ASTM C-1363 test method [ASTM 2006] and ASTM C-518 test method [ASTM 2007]). After gaining confidence in the present model, it was used to predict the R-values of the three residential 2 × 6 wood-frame wall specimens that were retrofitted using thermal insulations of XPS without VIP (W1, W2, and W3).

All R-values presented in this paper for different wall specimens are the surface-to-surface R-values. Figure 8 shows a comparison between the R-values for different wall specimens. As shown in this figure, the XPS retrofit wall assembly (W1) resulted in the lowest R-value (29.6 ft^2·h·°F/Btu); whereas the C-O VIP retrofit wall assembly (W2) resulted in

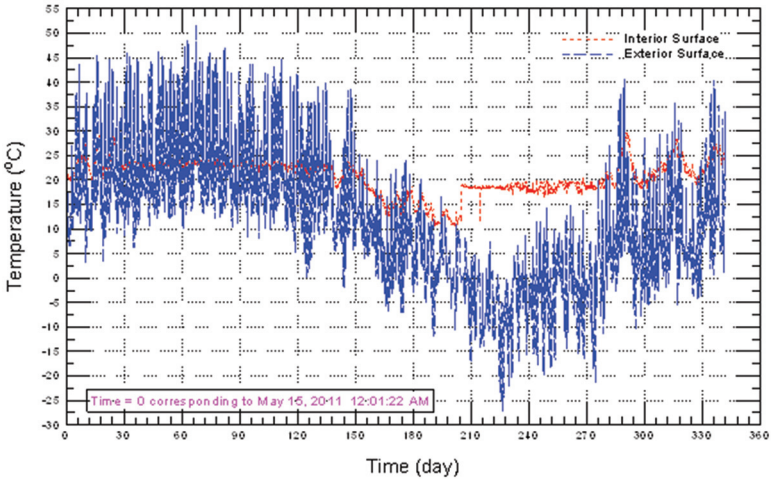

Figure 7 *Temperature measurements on the indoor and outdoor surfaces of the XPS retrofit wall assembly (W1).*

the highest R-value (55.4 $ft^2 \cdot h \cdot °F/Btu$). The R-value of the T&G VIP retrofit wall assembly, W3 (without furred-airspace) was 53.8 $ft^2 \cdot h \cdot °F/Btu$, which is lower than that for W2 by 1.58 $ft^2 \cdot h \cdot °F/Btu$. This means that the furred-airspace in the C-O VIP retrofit wall assembly (W2) having surface emissivity of all surfaces bounded in the airspace of 0.9 (ASHRAE 2009) contributed to the R-value by a value of 1.58 $ft^2 \cdot h \cdot °F/Btu$. However, installing foil with low emissivity on the surfaces of the furred-airspace would result in further enhancement of the thermal performance of the C-O VIP retrofit wall assembly.

As explained in Maref et al. (2012b), the test results of the C-O VIP retrofit wall specimen (W2) showed that one of the VIPs failed during normal operation (at time = 202 day). At time = 271 day, this VIP was subsequently replaced by a new VIP component once it became apparent that the expected thermal performance of the wall was not being achieved. The R-value of the failed VIP was measured using the ASTM C-518 test method (ASTM 2007) and found to reduce the R-value from 39.9 $ft^2 \cdot h \cdot °F/Btu$ to 3.32 $ft^2 \cdot h \cdot °F/Btu$ (a factor of ~12). Consequently, because there is always a risk of puncturing VIPs either during the installation process or over the course of its in-service use, a parametric study was conducted to predict the R-value of the wall assembly when one or more VIPs is punctured or failed by other means. Furthermore, because the VIP is more expensive than an XPS panel, this parametric analysis was conducted to determine the R-value when one or more VIPs is replaced by an XPS panel of the same dimension as that of the VIP. In these analyses, six cases were considered. These cases are shown in Figure 9a through Figure 9f for the T&G VIP wall specimen (W3). In Figure 9f, the case-VI represents the situation when the five VIPs in Figure 9a either failed or replaced by an XPS layer.

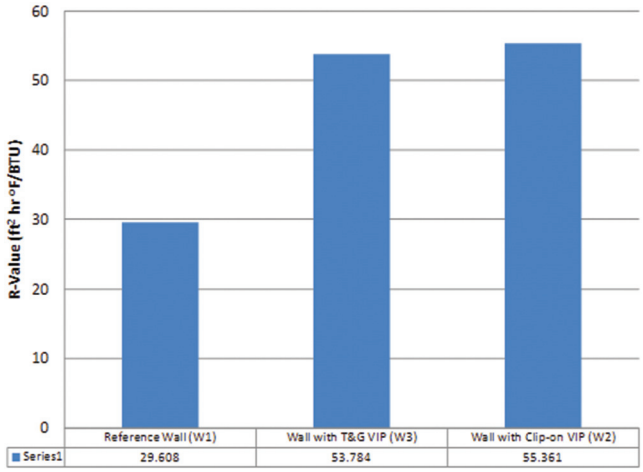

Figure 8 *Comparisons between the R-values of different wall specimens without considering the effect of thermal bridging due to the envelope of the VIPs.*

Comparisons of R-values of the T&G VIP wall specimen (W3) for case-I through case-VI (see Figure 9) when the VIP failed or replaced by an XPS layer are shown in Figure 10. This approach is similar to the approach by Nussbaumer et

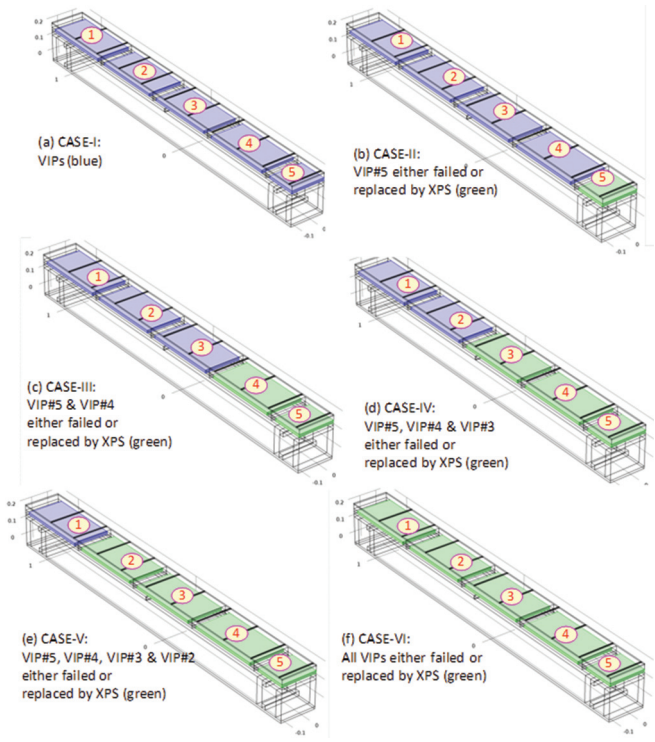

Figure 9 *Schematics of different cases when VIP either failed or replaced by XPS panel (see the green dashed boxes in Figures 2a, 2b, and 2c).*

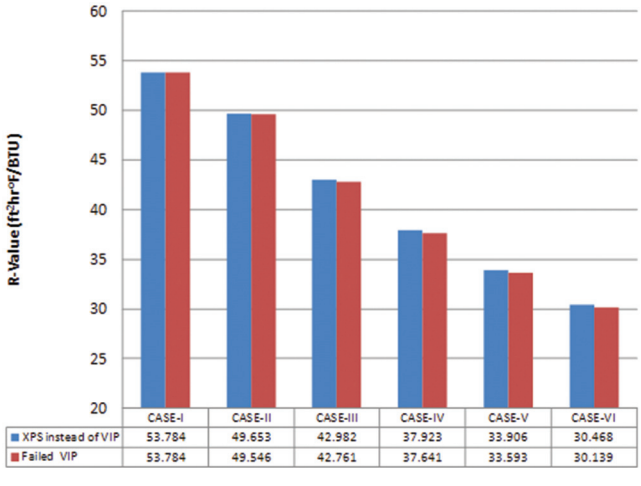

Figure 10 *Comparisons between R-values for case I through case VI (see Figure 9) of T&G VIP wall specimen (W3) without considering the effect of thermal bridging due to the envelope of the VIPs.*

al. (2006). Also, Table 1 shows the reduction in the R-values when the VIP failed or replaced by an XPS layer.

It is important to indicate that when all VIPs failed (case-VI, Figure 10), the R-value of the T&G VIP wall specimen (R = 30.139 $ft^2 \cdot h \cdot °F/Btu$) is only 1.8% higher than that for the reference wall (XPS retrofit wall specimen, R = 29.608 $ft^2 \cdot h \cdot °F/Btu$, see Figure 8). Therefore, consideration must be given when handling and installing VIPs for retrofitting wall specimens to minimize the risk of puncturing the VIP.

As indicated earlier, the measured thermal conductivity and R-value when the VIP failed were 0.0257 W/(m·K) and 3.32 $ft^2 \cdot h \cdot °F/Btu$, respectively. On the other hand, the R-value of an XPS layer (thermal conductivity = 0.029 W/[m·K] [ASHRAE 2009]) of the same thickness as VIP (15 mm thick) is 2.94 $ft^2 \cdot h \cdot °F/Btu$, which is approximately equal to the R-value of the VIP when it failed. As such, the reduction in the R-value when replacing VIP by XPS layer is approximately the same as when the VIP failed (see Figure 10). For example, for the situation when the VIP is replaced by XPS layer, Figure 10 and Table 1 show that the R-values are reduced by 8.3%, 25.1%, 41.8%, 58.6%, and 76.2% for case-II, case-III, case-IV, case-V, and case-VI, respectively, which are approximately the same as when the VIP failed. Hence, unless the VIP panel itself can be replaced, there is no benefit with respect to thermal performance of the overall assembly if replacing it with XPS panel. Note the effect of the thermal bridging due the envelope of VIP on the total R-values of the wall systems was not accounted for. The above comparisons between the performance of different wall specimens may change in the case of accounting for the effect of thermal bridging due to the VIP envelope.

Table 1. Comparisons Between R-Values for Case I through Case VI (see Figure 9) of T&G VIP Wall Specimen (W3)

	R-Value of Wall Assembly		Reduction % in R-Value Due to	
Case	Having Failed VIPs ($ft^2 \cdot h \cdot °F/Btu$)	Having VIPs Replaced by XPS ($ft^2 \cdot h \cdot °F/Btu$)	Failed VIPs	Replacing VIP by XPS
I	53.784	53.784	0%	0%
II	49.545	49.653	8.50%	8.30%
III	42.761	42.982	25.80%	25.10%
IV	37.641	37.923	42.90%	41.80%
V	33.593	33.906	60.10%	58.60%
VI	30.139	30.468	78.50%	76.20%

During the test period, it was noted that the VIP#2 in the C-O VIP wall specimen had failed at time = 202 day (Maref et al. 2012b; Saber et al. 2012e). Numerical simulations were conducted to predict the R-value for this situation for both the T&G VIP and the C-O VIP wall specimens. For T&G VIP wall specimen (R = 53.784 $ft^2 \cdot h \cdot °F/Btu$), Figure 11 shows that the R-value was reduced to R = 45.876 $ft^2 \cdot h \cdot °F/Btu$ in the case where VIP#2 only failed and R = 30.468 $ft^2 \cdot h \cdot °F/Btu$ when all VIPs were replaced by XPS layers (a reduction of 17.2% and 76.2%, respectively). Similarly, for the C-O VIP wall specimen, Figure 12 shows that the R-value (R = 55.361 $ft^2 \cdot h \cdot °F/Btu$) was reduced by 16.5% and 75.5% in the cases when VIP#2 failed (R = 47.503 $ft^2 \cdot h \cdot °F/Btu$) and when all VIPs were replaced by XPS layers (R = 31.545 $ft^2 \cdot h \cdot °F/Btu$), respectively.

DYNAMIC HEAT TRANSMISSION IN DIFFERENT WALL SPECIMENS

In order to validate the present model, and hence use it to determine the yearly heating and cooling loads of different wall specimens, transient numerical simulations were conducted for the three wall specimens (W1, W2, and W3). In these simulations, the initial temperature in all material layers of the wall specimens was assumed uniform and equal to 10.0°C. Because this initial temperature was not the same as that was recorded in the test, it was anticipated that the predicted dynamic response of the different wall specimens during the first period of the test (say the first 24–48 h) would be different than that obtained from the measurements. For the purpose of validating the present model, the indoor and outdoor surfaces for all wall

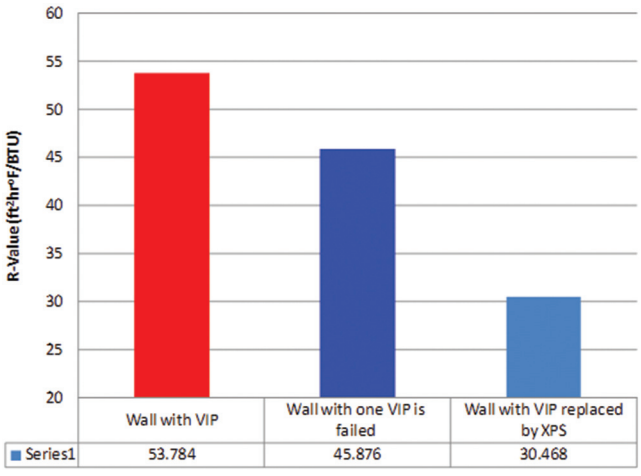

Figure 11 *Comparisons between R-values for case I, when VIP#2 failed, and all VIP were replaced by XPS (see Figure 9) of T&G VIP wall specimen (W3).*

systems were subjected to temperature boundary conditions. As an example, the temperatures on the outdoor and indoor surfaces of wall specimen W1 (changed with time) are shown in Figure 7. A description of all instrumentation and measurements are available in Maref et al. (2012b). In each wall system, three heat flux transducers (HFTs) were used to measure the heat flux at the middle (mid-height and mid-width) of each wall at three interfaces, namely (Maref et al. 2012b; Saber et al. 2012e):

- HFT1 at the cladding: XPS interface (cladding type: vinyl siding for W1, smart board for W2 and W3);

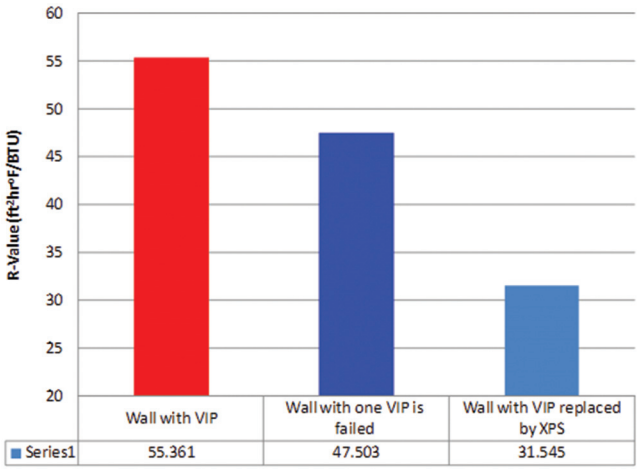

Figure 12 *Comparisons between R-values for case I, when VIP#2 failed, and all VIP were replaced by XPS (see Figure 9) of C-O VIP wall specimen (W2).*

- HFT2 at XPS: OSB interface; and
- HFT3 at polyethylene lapped air barrier: gypsum interface.

As an example, Figure 13 shows comparison between the measured and the predicted values of heat flux heat flux at the XPS/OSB interface during the test period for the wall specimen (W1). As shown in this figure, the predicted heat flux is in good agreement with the measurements. Furthermore, the detail comparisons between the predicted heat fluxes and measured heat fluxes at different layer interfaces as described above for the three wall specimens (W1, W2, and W3) are available elsewhere (Saber et al. 2012e). The results showed that both predicted and measured heat fluxes were in good agreements (see Saber et al. [2012e] for more details).

YEARLY CUMULATIVE HEATING AND COOLING LOADS

After the present model was validated, it was used to predict the yearly cumulative heating and cooling loads for different wall specimens and subjected to the climatic condition of Ottawa in the period between May 2011 and May 2012. As an example, Figure 14 shows the predicted heat flux on the indoor surface of the gypsum board for wall specimen W1. In this figure, positive values of heat flux represent the case when cooling loads are needed whereas negative values of heat flux, shown in this figure, represent the case when heating loads are needed. Note that the effect of thermal mass of all wall layers was accounted for. The negative and positive heat fluxes shown in this figure were used to calculate the cumulative energy loss (i.e., yearly

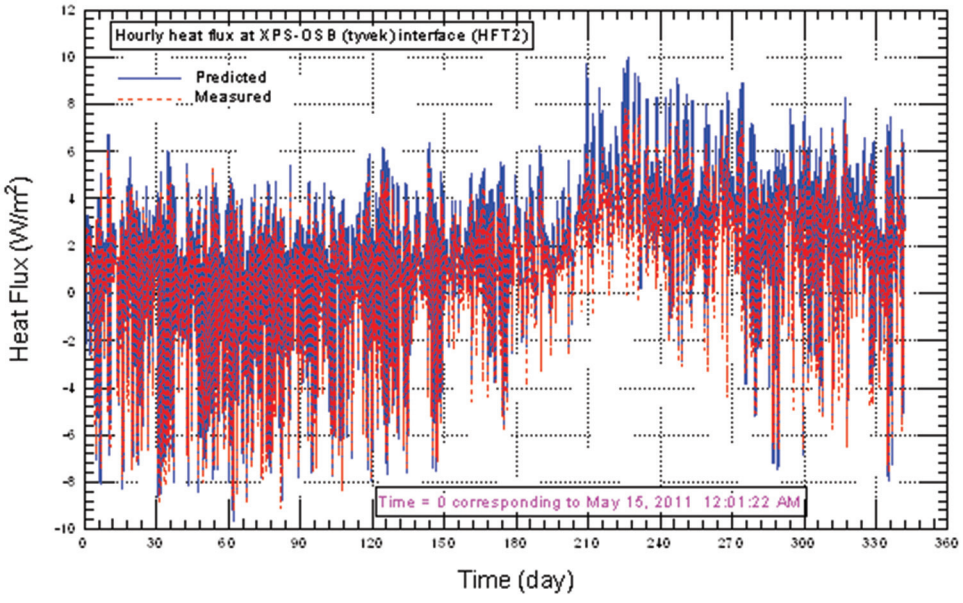

Figure 13 *Comparisons between predicted and measured heat fluxes at XPS/OSB interface for XPS retrofit wall specimen (W1).*

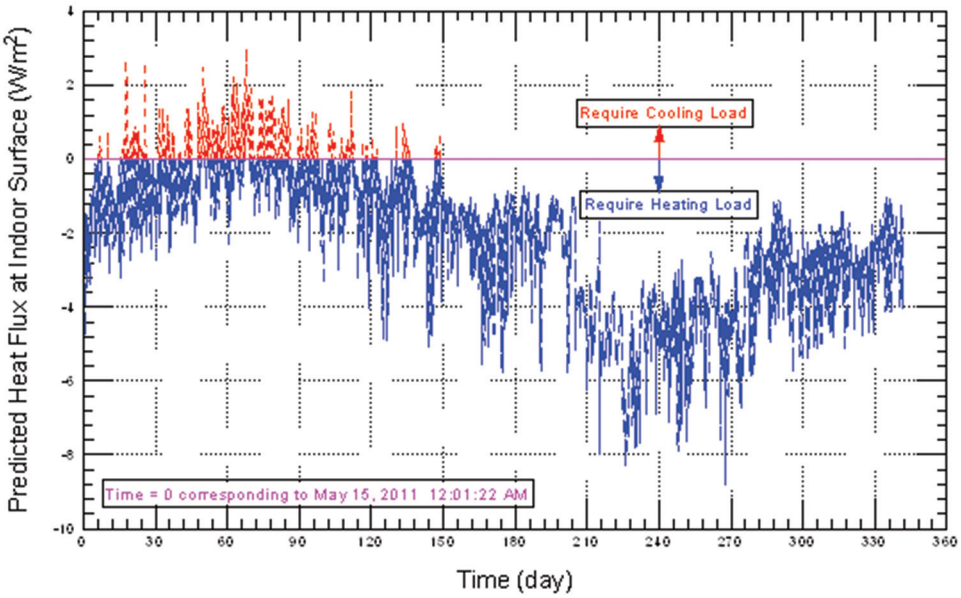

Figure 14 *Predicted heat flux at the indoor surface for XPS retrofit wall specimen (W1).*

heating load) and cumulative energy gain (i.e., yearly cooling load), respectively. The results obtained are shown in Figure 15. As shown in this figure, the yearly cooling loads were approximately the same for the different wall specimens given that over the test period which occurred over the summer season, the outdoor temperature was close to that of the indoor temperature. However, the yearly heating load for the XPS retrofit wall specimen (744 W·day/m^2) was 69.9% and 78.8%, respectively, higher than that for the T&G VIP retrofit wall specimen (438 W·day/m^2), and the C-O VIP retrofit wall specimen (416 W·day/m^2).

By comparing the wall specimens that were retrofitted with VIPs, the effect of the furred-airspace assembly in the C-O VIP retrofit wall specimen when the emissivity of all surfaces bounding the airspace was 0.9 (ASHRAE 2009) resulted in a reduction in the yearly heating load by 5.0% compared to the T&G VIP retrofit wall specimen without furred-airspace assembly.

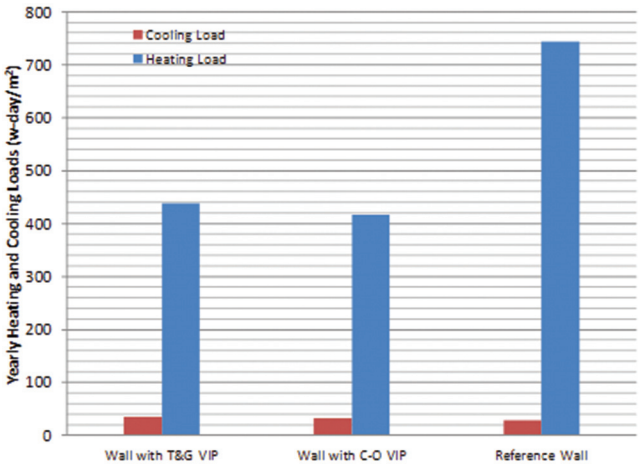

Figure 15 *Comparisons of the predicted yearly cumulative heating and cooling loads of different wall specimens.*

CONCLUDING REMARKS

To maintain reasonable envelope thickness while having high thermal performance, a promising recent innovation in building technology was investigated within the context of its application using vacuum insulation panel (VIP) systems. This concept is gaining interest and is being considered by architects and building practitioners for new and retrofit construction. In this study, steady-state and transient numerical simulations were conducted to predict the thermal performance of residential 2 × 6 wood-frame wall specimens that were retrofitted using vacuum insulation panels (VIPs) (W2 and W3) and extruded polystyrene foam, XPS (W1). Numerical simulations were conducted in order to investigate the effect of the thermal bridging due to the envelope of the VIP on its effective R-value. Depending on the VIP size, and the thickness of VIP envelope and its thermal conductivity, the results showed that the thermal bridging due the VIP envelope can have a significant effect on its effective R-value. This effect, however, was neglected in this study due to lack of information about the envelope of the VIP.

In order to determine the R-values of different wall specimens, steady-state numerical simulations were conducted using the same outdoor and indoor conditions as described in the standard test method using guarded hot box (GHB) (in accordance of the ASTM C-1363 [ASTM 2006]). Results showed that the XPS retrofit wall specimen resulted in the lowest R-value (29.6 ft^2·h·°F/Btu) while the C-O VIP

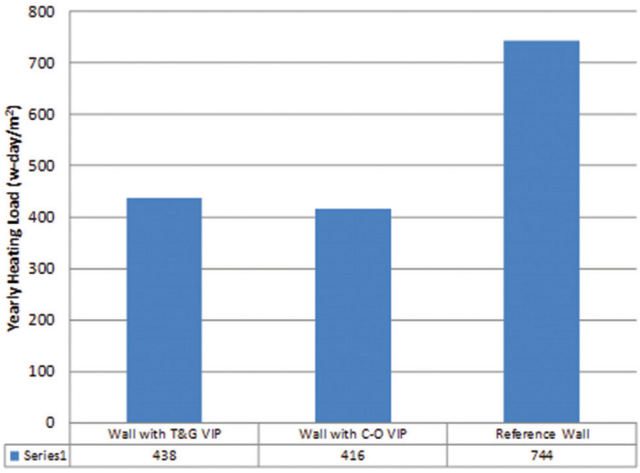

Figure 16 *Comparisons of yearly cumulative heating load of different wall specimens.*

retrofit wall specimen resulted in the highest R-value (55.4 $ft^2 \cdot h \cdot °F/Btu$). The R-value of the T&G VIP retrofit wall specimen (without furred-airspace) was 53.8 $ft^2 \cdot h \cdot °F/Btu$, which was lower than that for C-O VIP retrofit wall specimen (with furred-airspace) by 1.58 $ft^2 \cdot h \cdot °F/Btu$. Furthermore, because there is a risk of the VIP to fail either during the installation process or during in-service conditions, a parametric study was conducted to predict the R-value when one or more VIPs failed.

In the second part of this study, transient numerical simulations were conducted in order to validate the present model and then determine the yearly heating and cooling loads for different wall specimens. The numerical results of heat fluxes were compared with the measured values of heat fluxes. The results showed that the comparison between the present model predictions and experimental data were in good agreement. After the present model was validated, it was used to determine the yearly heating loads for different wall specimens. Results showed that the yearly heating loads for the XPS retrofit wall specimen (744 $W \cdot day/m^2$) was 69.9% and 78.8%, respectively, greater than that for the T&G VIP retrofit wall specimen (438 $W \cdot day/m^2$) and the C-O VIP retrofit wall specimen (416 $W \cdot day/m^2$). For the wall specimens that were retrofitted with VIPs, the effect of the furred-airspace in the C-O VIP retrofit wall specimen when the emissivity of all surfaces that bounded the airspace was 0.9 resulted in a reduction in the yearly heating load by 5.0% compared to the T&G VIP retrofit wall specimen without furred-airspace. It is important to mention that the conclusion of this paper may change when the effect of thermal bridging due to the VIP envelope is significant. In general, research study on VIPs should continue in order to improve thermal resistance by reducing, for example, thermal bridging due to the VIP envelope and improving the way that it is manufactured. By considering the center of the panel, VIPs are of interest owing to their exceptional insulating R-value, up to 10.6 $m^2 \cdot K/W$ (60 $ft^2 \cdot h \cdot °F/Btu$) per inch or even higher.

ACKNOWLEDGMENTS

The authors wish to thank Mr. S. Plescia from the Canada Mortgage and Housing Corporation (CMHC) and Mr. A. Parekh from the Natural Resources Canada (NRCan) for providing guidance and funding for this project. Our thanks are also extended to P. Mukhopadhyaya and D. van Reenen for their support.

REFERENCES

Armstrong, M., H.H. Saber, W. Maref, M.Z. Rousseau, G. Ganapathy, G., and M.C. Swinton. 2011a. Field energy performance of an insulating concrete form (ICF) wall. 13th CCBST conference, The 13th Canadian Conference on Building Science and Technology, Winnipeg, Manitoba May 10 – 13, 2011.

Armstrong, M., W. Maref, H.H. Saber, M.Z. Rousseau, G. Ganapathy, and M.C. Swinton. 2011b. The impact of the thermal mass on field energy performance of insulating concrete form (ICF) wall. International Workshop on Whole Building Testing, Evaluation and Modelling for Energy Assessment, Copenhagen, Denmark, May 18, 2011, pp. 1–12.

ASTM Designation: C 1130-07. 2009. *Standard Practice for Calibrating Thin Heat Flux Transducers*. Annual Book of ASTM Standards, sec 4, Construction, vol. 04.06, Thermal Insulation; Building & Environment Acoustic, pp. 577–584.

ASTM Designation: C-518-04. 2007. *Steady-State Thermal Transmission Properties by Means of the Heat Flow Meter Apparatus*. Section 4, Volume 04.06, Thermal Insulation, 2007 Book of ASTM Standards.

ASHRAE. 2009. *ASHRAE Handbook—Fundamentals* (SI), Chapter 26, Atlanta: ASHRAE.

ASTM. 2006. ASTM C-1363, *Standard Test Method for the Thermal Performance of Building Assemblies by Means of a Hot Box Apparatus*. 2006 Annual Book of ASTM Standards 04.06:717-59.

Binz, A., and G. Steinke. 2005. Applications of vacuum insulation in the building sector. *7th International Vacuum Insulation Symposium Proceedings*, EMPA, Duebendorf, Zurich, Switzerland, September 28–29, 2005, pp. 43–48.

Brunner, S., and H. Simmler. 2008. In situ performance assessment of vacuum insulation panels in a flat roof construction. *Vacuum* 82:700–707.

Cremers, J.M., 2005. Typology of applications for opaque and translucent VIP in the building envelope and their potential for temporary thermal insulation. *7th International Vacuum Insulation Symposium Proceedings*, pp. 189–196, EMPA, Duebendorf, Zurich, Switzerland, September 28–29, 2005.

Elmahdy, A.H., M. Maref, H.H. Saber, M.C. Swinton, and R. Glazer. 2010. Assessment of the energy rating of insulated

wall assemblies a step towards building energy labeling. 10th International Conference for Enhanced Building Operations (ICEBO2010), Kuwait, October 2010.

Elmahdy, A.H., W. Maref, M.C. Swinton, H.H. Saber, and R. Glazer. 2009. Development of energy ratings for insulated wall assemblies. Building Envelope Symposium, San Diego, California, October 26, 2009, 21–30.

Haavi, T., B.P. Jelle, and A. Gustavsen. 2012. Vacuum insulation panels in wood frame wall constructions with different stud profiles. *Journal of Building Physics* 36: 212–226.

Ghazi Wakili, K., R. Bundi, and B. Binder. 2004. Effective thermal conductivity of vacuum insulation panels. *Building Research and Information* 32:293–299.

HiPTI-High Performance Thermal Insulation, IEA /ECBCS Annex 39. 2005. Vacuum insulation in the building sector: systems and applications. Subtask A and B.

Maref, W., H.H. Saber, M.M. Armstrong, R. Glazer, G. Ganapathy, M. Nicholls, H. Elmahdy, and M.C. Swinton. 2012a. Integration of vacuum insulation panels into Canadian wood frame walls, Report I: Performance assessment in the laboratory, Internal Research Report, Building Envelope Engineering Materials Program, Construction Portfolio, National Research Council of Canada, Ottawa, Canada.

Maref, W., H.H. Saber, G. Ganapathy, and M. Nicholls 2012b. Field energy performance and hygrothermal evaluation of different strategies of energy retrofit for residential wood-frame wall systems field using VIP, Part I—Field monitoring and thermal performance, Internal Research Report, Construction Portfolio, National Research Council of Canada, Ottawa.

Maref, W. 2011. Program of Energy Research and Development – PERD. Internal Communication.

Maref, W., H.H. Saber, R. Glazer, M.M. Armstrong, M. Nicholls, H. Elmahdy, and M.C. Swinton. 2011. Energy performance of highly insulated wood-frame wall systems using a VIP. 10th International Vacuum Insulation Symposium (Ottawa, Ontario 2011-09-15), 68–76.

Maref, W., M.K. Kumaran, M.A. Lacasse, M.C. Swinton, and D. van Reenen. 2002. Laboratory measurements and benchmarking of an advanced hygrothermal model. *Proceedings of the 12th International Heat Transfer Conference*, Grenoble, France, August 18, 2002, pp. 117–122.

Mukhopadhyaya, P. 2010. High-performance thermal insulation—better than ever. *Solplan Review* (153), pp. 1–3.

Mukhopadhyaya, P., 2006. High performance vacuum insulation panel-research update from Canada. *Global Insulation Magazine*, pp. 9–15, NRCC-48705.

Mukhopadhyaya, P., M.K. Kumaran, N. Normandin, D. van Reenen, and J.C. Lackey. 2009. Fiber-powder composite as core material for vacuum insulation panel. 9th International Vacuum Insulation Symposium, London, UK, September 17–18, 2009, pp. 1–9.

Mukhopadhyaya, P., M.K. Kumaran, N. Normandin, D. van Reenen, and J.C. Lackey. 2008. High performance vacuum insulation panel: Development of alternative core materials. *Journal of Cold Regions Engineering* 22(4): 103–123.

Nussbaumer, T., K. Ghazi Wakili, and Ch. Tanner. 2006. Experimental and numerical investigation of the thermal performance of a protected vacuum-insulation system applied to a concrete wall. *Applied Energy* 83:841–855.

Ogden, R., and C. Kendrick. 2005. VIP cladding panels for buildings: Applications and conceptual solutions. *7th International Vacuum Insulation Symposium Proceedings*, pp. 153–160, EMPA, Duebendorf, Zurich, Switzerland, September 28–29, 2005.

Rogatzki, P. 2009. Pre-fabricated cavity walls-the potential for vacuum insulated panels. 9th International Vacuum Insulation Symposium, September 17–18, 2009, pp. 1–26.

Saber, H.H. 2013. Thermal performance of wall assemblies with low emissivity. *Journal of Building Physics* 36(3):308–329.

Saber, H.H. 2012. Investigation of thermal performance of reflective insulations for different applications. *Journal of Building and Environment* 52:32–44.

Saber, H.H., and W. Maref. 2012. Effect of furring orientation on thermal response of wall systems with low emissivity material and furred-airspace. The Building Enclosure Science & Technology (BEST3) Conference, Atlanta, Georgia, USA, April 2–4, 2012.

Saber, H.H., W. Maref, H. Elmahdy, M.C. Swinton, and R. Glazer. 2012a. 3D heat and air transport model for predicting the thermal resistances of insulated wall assemblies. *Journal of Building Performance Simulation* 5(2): 75–91, (NRCC-53583).

Saber, H.H., W. Maref, and M.C. Swinton. 2012b. Thermal response of basement wall systems with low emissivity material and furred airspace. *Journal of Building Physics* 35(2):353–371, (NRCC-53962).

Saber, H.H., W. Maref, G. Sherrer, and M.C. Swinton. 2012c. Numerical modelling and experimental investigations of thermal performance of reflective insulations. *Journal of Building Physics* 36(2):163–177.

Saber, H.H., M.C. Swinton, P. Kalinger, and R.M. Paroli. 2012d. Long-term hygrothermal performance of white and black roofs in North American climates. *Journal of Building and Environment*, 50:141–154.

Saber, H.H., W. Maref, and G. Ganapathy. 2012e. Field energy performance and hygrothermal evaluation of different strategies of energy retrofit for residential wood-frame wall systems using VIP, Part – II: Model benchmarking and numerical simulations. Internal Research Report, National Research Council of Canada, Ottawa.

Saber, H.H., and A. Laouadi, 2011. Convective heat transfer in hemispherical cavities with planar inner surfaces (1415-RP). *Journal of ASHRAE Transactions*, Volume 117, Part 2, 2011.

Saber, H.H., W. Maref, M.C. Swinton, and C. St-Onge. 2011a. Thermal analysis of above-grade wall assembly with low emissivity materials and furred-airspace. *Journal of Building and Environment*, 46(7):1403–1414.

Saber, H.H., M.C. Swinton, P. Kalinger, and R.M. Paroli. 2011b. Hygrothermal simulations of cool reflective and conventional roofs. 2011 NRCA International Roofing Symposium, Emerging Technologies and Roof System Performance, Washington D.C., USA, Sept. 7–9, 2011.

Saber, H.H., W. Maref, M.M. Armstrong, M.C. Swinton, M.Z. Rousseau, and G. Ganapathy. 2011c. Numerical simulations to predict the thermal response of insulating concrete form (ICF) wall in cold climate. Research Report-310, NRC Institute for Research in Construction.

Saber, H.H., and M.C. Swinton, 2010. Determining through numerical modeling the effective thermal resistance of a foundation wall system with low emissivity material and furred – airspace. International Conference on Building Envelope Systems and Technologies, ICBEST 2010, Vancouver, Canada, June 27–30, 2010.

Saber, H.H., W. Maref, A.H. Elmahdy, M.C. Swinton, and R. Glazer. 2010a. 3D thermal model for predicting the thermal resistances of spray polyurethane foam wall assemblies. Building XI conference, Clearwater, Florida, December 2010.

Saber, H.H., W. Maref, M.A. Lacasse, M.C. Swinton, and K. Kumaran. 2010b. Benchmarking of hygrothermal model against measurements of drying of full-scale wall assemblies. International Conference on Building Envelope Systems and Technologies, ICBEST 2010, Vancouver, Canada, June 27–30, 2010.

Saber, H.H., W. Maref, M.M. Armstrong, M.C. Swinton, M.Z. Rousseau, and G. Ganapathy. 2010c. Benchmarking 3D thermal model against field measurement on the thermal response of an insulating concrete form (ICF) wall in cold climate. Eleventh International Conference on Thermal Performance of the Exterior Envelopes of Whole Buildings XI, Clearwater, FL, USA, December 4–9, 2010.

Schwab, H., U. Heinemann, A. Beck, H.P. Ebert, and J. Fricke. 2005. Dependence of thermal conductivity on water content in vacuum insulation panels with fumed silica kernels. *Journal of Thermal Envelope and Building Science* 28:319–326.

Simmler, H., and S. Brunner. 2005a. Aging and service life of VIP in buildings. *7th International Vacuum Insulation Symposium Proceedings*, pp. 15–22, EMPA, Duebendorf, Zurich, Switzerland, September 28–29, 2005.

Simmler, H., and S. Brunner. 2005b. Vacuum insulation panels for building application basic properties, aging mechanisms and service life. *Energy and Buildings* 37: 1122–1131.

Stahl, Th., S. Brunner, M. Zimmermann, and K. Ghazi Wakili. 2012. Thermo-hygric properties of a newly developed aerogel based insulation rendering for both exterior and interior applications. Short communication, *Energy and Buildings* 44:114–117.

Xiaobo, D., G. Yimin, B. Chonggao, H. Yongnian, and X. Zhen'gang. 2013. Optimization of glass fiber based core materials for vacuum insulation panels with laminated aluminum foils as envelopes. *Vacuum* 97:55–59.